Article

Journal of
Nanoscience and Nanotechnology
Vol. 15, 1269–1279, 2015
www.aspbs.com/jnn

All-Electron Scalar Relativistic Calculations on the Adsorption of Small Gold Clusters Toward Methanol Molecule

Xiang-Jun Kuang[1, 2, *], Xin-Qiang Wang[2], and Gao-Bin Liu[2]

[1] School of Science, Southwest University of Science and Technology, Mianyang, Sichuan, 621010, China
[2] College of Physics, Chongqing University, Chongqing, 400044, China

Under the framework of DFT, an all-electron scalar relativistic calculation on the adsorption of Au_n ($n = 1$–13) clusters toward methanol molecule has been performed with the generalized gradient approximation at PW91 level. Our calculation results reveal that the small gold cluster would like to bond with oxygen of methanol molecule at the edge of gold cluster plane. After adsorption, the chemical activities of hydroxyl group and methyl group are enhanced to some extent. The even-numbered Au_nCH_3OH cluster with closed-shell electronic configuration is relatively more stable than the neighboring odd-numbered Au_nCH_3OH cluster with open-shell electronic configuration. All the Au_nCH_3OH clusters prefer low spin multiplicity ($M = 1$ for even-numbered Au_nCH_3OH clusters, $M = 2$ for odd-numbered Au_nCH_3OH clusters) and the magnetic moments are mainly contributed by gold atoms. The odd-even alterations of magnetic moments and electronic configurations can be observed clearly and may be simply understood in terms of the electron pairing effect.

Keywords: Gold Clusters, Methanol Molecule, Adsorption, All-Electron Scalar Relativistic Calculations.

1. INTRODUCTION

Methanol is predicted to be an important component in the next generation of renewable green fuels, and there has recently been interest in the use of methanol in fuel cells.[1–3] Small transitional metal clusters usually have very distinct catalytic properties from the counterpart bulk materials because of the quite large surface-to volume ratio, the methanol may be produced using transition metal cluster catalysts, so there is considerable interest in better understanding the interaction between transition metal cluster and methanol molecule during methanol synthesis to improve the efficiency of the reactions.[4–16]

Among all transition metal cluster catalysts, nano-sized gold clusters, as a new kind of catalyst to reduce air pollution, have attracted considerable interest recently from both industrial and scientific communities[17–23] since Haruta discovered the CO oxidation catalyzed by supported gold clusters in 1989.[24] Experimental and theoretical studies have proved that free and supported nano-sized gold clusters can efficiently catalyze the CO, NO and H_2 oxidation reaction at low temperature.[25–31] Along this line, some studies on the interaction between gold clusters and methanol molecule had been undertaken in order to investigate the catalytic properties of gold cluster toward methanol.[32–36] By using density functional theory (DFT) within the generalized gradient approximation (GGA), the structural, energetic, and electronic properties of $Au_3^+(CH_3OH)_m$ ($m = 1$–3) and $Au_5^+(CH_3OH)_m$ ($m = 1$–5) have been investigated.[32] The calculation results of geometric parameters, vibrational frequencies, adsorption energies and Mulliken charges show that more than one methanol molecule can be adsorbed onto small clusters of gold ions. The red shift of the C—O stretching frequency decreases as the number of methanol molecules increases or as gold cluster size increases. The positive charge on $Au_{3,5}^+$ and coordination number of the adsorption sites on the gold cluster are the dominant factors responsible for the strength of the interactions. Structural, dynamical, and electronic properties of adducts obtained by adsorbing one methanol molecule onto charged and neutral gold clusters had been investigated using Car–Parrinello *ab initio* molecular dynamics.[33] The absorption process occurs by the formation of Au—O coordination bond to one particular gold atom without altering the structure of the

*Author to whom correspondence should be addressed.

 1533-4880/2015/15/1269/011 doi:10.1166/jnn.2015.9044

underlying cluster. This chemical bond is much stronger for the charged gold clusters than for the neutral gold clusters. In the charged case, the C—O stretching vibration of the interacting methanol molecule is found to increase discontinuously as the underlying cluster structure changes from two-dimensional to three-dimensional. The weaker C—O bond in the neutral species however has "insufficient strength" to be sensitive to changes in coordination number and cluster structure. This leads to a constant C—O stretching frequency as the size of the cluster increases, including the regime where the gold cluster changes from planar to three-dimensional. Meanwhile, using the infrared photodissociation of trapped $Au_n^+(CH_3OH)_m$, the adducts of up to three CH_3OH molecules on charged gold clusters had been studied.[34] Storage and size selection of $Au_n^+(CH_3OH)_m$ in a penning trap allows to perform IR photofragmentation experiments on well defined species. Desorption of CH_3OH is induced by excitation of the C—O stretching vibration. Its frequency is red shifted with respect to the gas phase value of methanol. The red shift decreases with increasing cluster size n and is related to a 2D → 3D shape transition in the region of $n = 7$–9. The red shift also decreases with increasing number of adsorbed methanol molecules. From the number of absorbed IR photons the separation energy of CH_3OH is estimated. For $n > 3$ size independent values of 0.5–0.7 eV are observed. Similarly, in order to probe cluster structures with sensor molecules, structural, dynamical and electronic properties of the adducts formed by adsorbing methanol onto size-selected gold clusters were investigated using infrared multiple-photon dissociation spectroscopy of trapped $Au_n^+CH_3OH$, $n \leq 15$, in conjunction with Car–Parrinello calculations.[35] The cluster–molecule interaction is mediated via a direct Au—O bond between one Au atom of the gold cluster and the methanol molecule. The adsorption site Au turns out to be the lowest-coordinated gold atom that is available in each cluster, which is two for the 2D ($n \leq 7$) and three or four for the 3D ($n \geq 9$) clusters. This goes hand in hand with the dimensionality change of the cluster structure at $n \leq 7$. No clear discontinuous relationship between the cluster–methanol bond distance and the change of dimensionality can be found. By far the longest distance 2.17 Å is found for the more weakly bound neutral Au_4CH_3OH adduct. In this case, the cluster–molecule interaction is too weak to turn the molecule into a sensor of the cluster's structure.

Even though some previous works can be found above, the information for the adsorption of gold cluster toward methanol molecule is still incomplete. Furthermore, in all these previous works, few are available to consider the influence of scalar relativistic effect. The reason for the preference of planar structures by gold clusters up to large size may be attributed to the scalar relativistic effects that cause the shrinking of the size of s orbitals, and thus enhance the s–d hybridization.[37–40] This phenomenon is most strikingly evident in gold cluster and called "gold maximum."[40] Our previous works also indicated that the scalar relativistic effect may have obvious influence on the adsorption behavior of gold clusters toward carbon monoxide and hydrogen molecules,[41,42] so it is necessary to include scalar relativistic effect in the study of interaction between gold clusters and methanol molecule. In this paper, under the framework of DFT, we shall perform an all-electron scalar relativistic (AER) calculation on the adsorption of gold clusters toward methanol molecule with the generalized gradient approximation (GGA) at PW91 level. The exploration of the structure of these clusters may help to understand the catalytic activity of gold cluster catalyst and the influence of scalar relativistic effects on the interaction between gold cluster and methanol molecule.

2. COMPUTATIONAL METHOD AND CLUSTER MODEL

All calculations are carried out with the DMOL 3 program package.[43,44] A double-numeric quality basis set with polarization functions (DNP) is chosen to describe the electronic wave functions. Within the generalized gradient approximation (GGA), the Perdew–Wang 91 exchange-correlation (XC) functional (PW91),[45] combined with the DFT-basis all-electron treatment and scalar or spin-orbit all-electron relativistic pseudopotentials[46] is used in the calculations. This scheme is a good compromise between accuracy and computational effort, and its application has been shown to be effective for many species including complexes formed by the adsorption of gold cluster toward small molecules.[47–50]

The initial structures of Au_nCH_3OH clusters can be got by the following way: First, referring to previous works on the configurations of pure Au_n clusters[51,52] and calculating some other structures of pure Au_n clusters including 3D geometries, we obtain the lowest energy geometries and related calculation data of pure Au_n clusters. Then, on the basis of the optimized equilibrium geometries of pure Au_n clusters, the initial structures of Au_nCH_3OH clusters are obtained by making CH_3OH molecule approach to each nonequivalent adsorption site of Au_n cluster molecularly, including all possible bonding patterns. All these initial structures are fully DFT optimized by relaxing the atomic positions until the force acting on each atom vanish (typically $F_i \leq 0.002$ Ha/Å).

To test the reliability of our calculations, the Au_2 dimer and CH_3OH molecule are calculated. The calculated Au—Au bond-length, the highest vibrational frequencies of Au—Au mode, and vertical ionization potentials for Au_2 dimer are 2.487 Å, 183.1 cm^{-1}, 9.370 eV, respectively. These results are in good agreement with the experimental values of 2.471 Å, 190.9 cm^{-1}, 9.200 eV for Au_2 cluster.[53–56] Furthermore, for free CH_3OH molecule, the calculated C—O, C—H, and O—H bond-lengths are 1.430 Å, 1.100 Å and 0.960 Å, respectively (see Fig. 1). These results are completely consistent with experimental

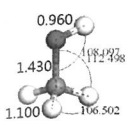

C_s, $^1\Sigma_g$

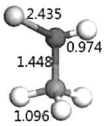

C_1, ^2A_g, $\Delta E = 0$

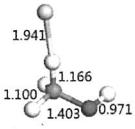

C_1, ^2B_g, $\Delta E = 0.067$ eV

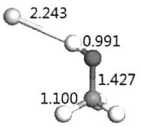

C_1, $^2\Sigma_g$, $\Delta E = 0.142$ eV

$D_{\infty h}$, $^1\Sigma_g$

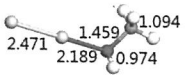

C_1, ^1A_g, $\Delta E = 0$

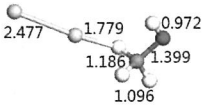

C_1, ^1B_g, $\Delta E = 0.368$ eV

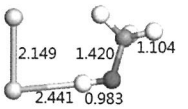

C_1, ^1B_g, $\Delta E = 0.684$ eV

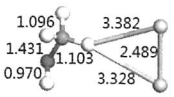

C_1, $^2\Sigma_g$, $\Delta E = 0.981$ eV

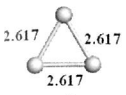

D_{3h}, $^2B_2$

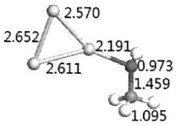

C_1, ^2A_g, $\Delta E = 0$

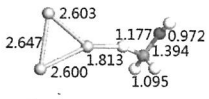

C_1, ^2B_g, $\Delta E = 0.373$ eV

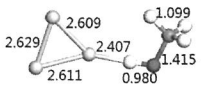

C_1, ^2B_g, $\Delta E = 0.752$ eV

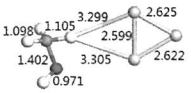

C_1, ^2B_g, $\Delta E = 0.913$ eV

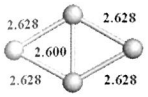

C_{2v}, ^1A_g

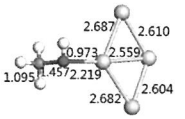

C_1, ^1A_g, $\Delta E = 0$

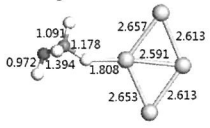

C_1, ^1A_g, $\Delta E = 0.335$ eV

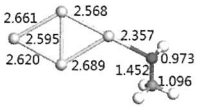

C_1, ^1A_g, $\Delta E = 0.366$ eV

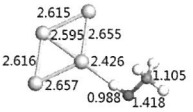

C_1, ^1A_g, $\Delta E = 0.617$ eV

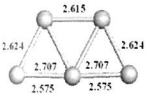

C_{2v}, $^2B_2$

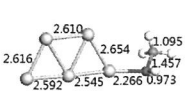

C_1, ^2A_g, $\Delta E = 0$

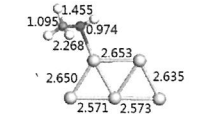

C_1, ^2A_g, $\Delta E = 0.102$ eV

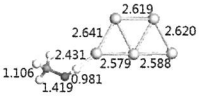

C_1, ^2A_g,$\Delta E = 0.561$ eV

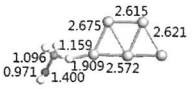

C_1, ^2B_g, $\Delta E = 0.784$ eV

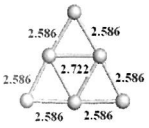

D_{3h}, $^1B_2$

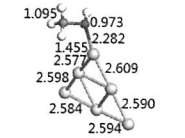

C_1, $^1A_1$, $\Delta E = 0$

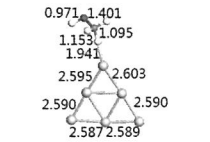

C_1, ^1A_g, $\Delta E = 0.158$ eV

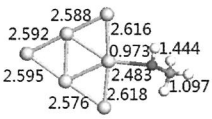

C_1, ^1A_g, $\Delta E = 0.304$ eV

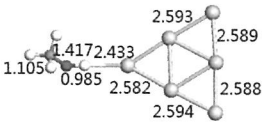

C_1, ^1A_g, $\Delta E = 0.379$ eV

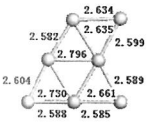

C_s, ^2A_g

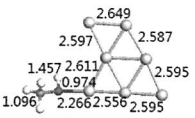

C_1, ^2A_g, $\Delta E = 0$

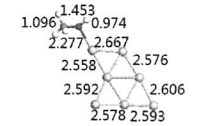

C_1, ^2A_g, $\Delta E = 0.110$ eV

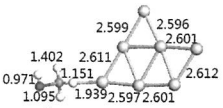

C_1, ^2A_g, $\Delta E = 0.295$ eV

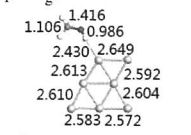

C_1, ^2A_g, $\Delta E = 0.326$ eV

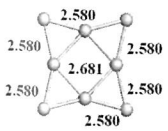

D_{4h}, $^1B_{2g}$

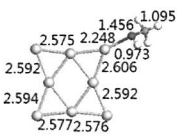

C_1, ^1A_g, $\Delta E = 0$

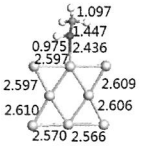

C_1, ^1B_g, $\Delta E = 0.164$ eV

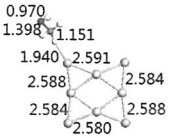

C_1, ^1A_g, $\Delta E = 0.322$ eV

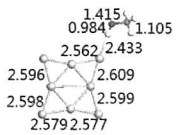

C_1,^1A_g,$\Delta E = 0.439$ eV

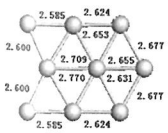

C_{2V}, $^2A_1$

C_1, ^2A_g, $\Delta E = 0$

C_1, ^2B_g, $\Delta E = 0.098$ eV

C_1, ^2A_g, $\Delta E = 0.211$ eV

C_1, ^2A_g, $\Delta E = 0.319$ eV

D_{2h}, $^1B_{2g}$

C_1, ^1A_g, $\Delta E = 0$

C_1, ^1A_g, $\Delta E = 0.091$ eV

C_1, ^1A_g, $\Delta E = 0.255$ eV

C_1, ^1A_g, $\Delta E = 0.311$ eV

Figure 1. Continued.

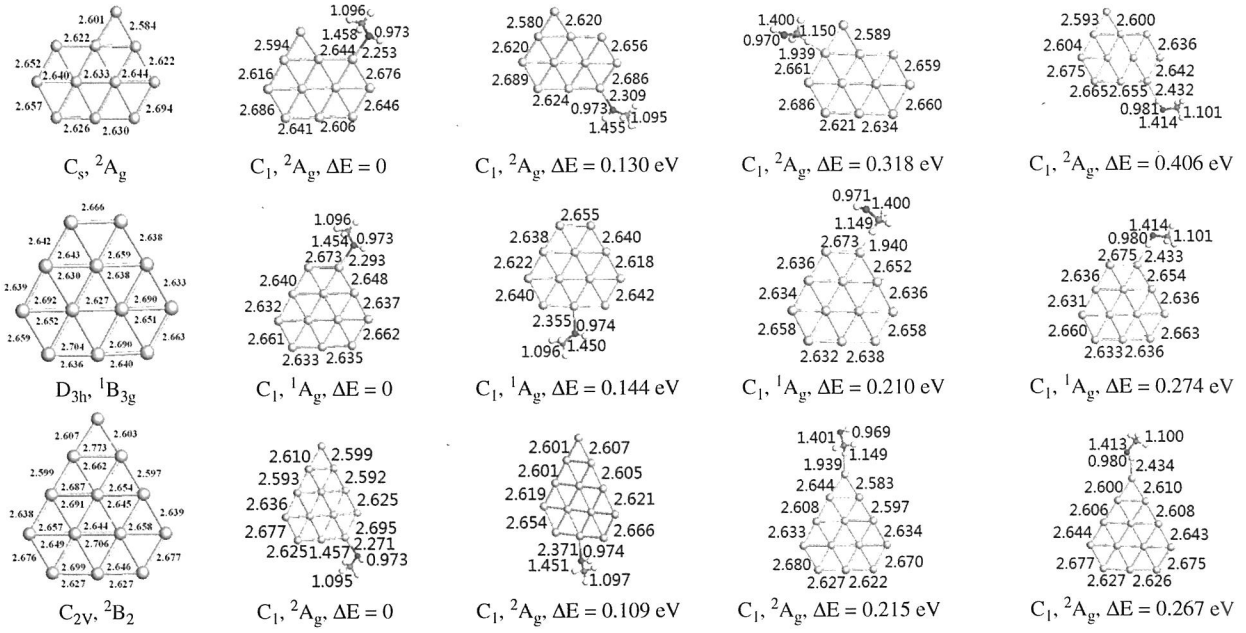

Figure 1. Optimized geometries for pure Au_n (n = 1–13) clusters and Au_nCH_3OH (n = 1–13) clusters. The bond lengths in angstrom, symmetry, electronic state and energy differences between the lowest energy geometry and its isomers are shown next to each cluster. The average Cu–Cu distances in nanometer are shown next to each cluster.

values.[57,58] Additionally, the calculated vibrational frequency of O-H mode is 3766.6 cm^{-1}, it is also close to the experimental values of 3681.0 cm^{-1}.[59] Therefore, the calculation method employed in this work is reliable and accurate enough.

3. RESULTS AND DISCUSSION

3.1. Geometrical Structures

Based on the lowest energy geometries of pure Au_n (n = 2–13) clusters depicted in Figure 1, an extensive lowest energy structures search for CH_3OH adsorption onto small gold clusters has been performed according to the way described in Section 2. The fully DFT optimized geometries of Au_nCH_3OH (n = 1–13) clusters including some low-lying geometric isomers with higher energies and the single CH_3OH molecule are also depicted in Figure 1 comparatively. Examining the lowest energy structures of Au_nCH_3OH clusters, the CH_3OH molecule prefers to occupy the on-top and single fold coordination site, and the small gold cluster would like to bond with oxygen rather than carbon or hydrogen. The adsorption site locates at the edge of gold cluster plane, the gold atom bonding with oxygen atom is singly coordinated with its neighbors at n = 2, doubly coordinated with its neighbors at n = 3, 5–9, and triply coordinated with its neighbors at n = 4, 10–13, respectively. After adsorption, the Au_n structures are only distorted slightly and still keep the planar structures. This situation also can be seen in some previous works[47–50,60,61] and one important consensus is that the reason for the planar structures and the delocalization of frontier molecular orbitals in pure small gold clusters may be attributed to the strong scalar relativistic effects.[37–40] The obvious delocalization of HOMO still can be observed clearly after adsorption (see Fig. 10). It is suggested that the scalar relativistic effect may play an important role in the properties of Au_nCH_3OH clusters and the maintenance of planar structures in Au_n parts might be the reflection of strong scalar relativistic effects. In all these lowest energy structures, the CH_3OH molecule reorients itself so as to adjust its center of mass lying on the same plane of gold cluster. In methyl group, one hydrogen atom locates in the same plane of gold cluster, and other two hydrogen atoms locate in the two side of Au_n—O plane perpendicularly. In hydroxyl group, the hydrogen atom locates in the same plane of gold cluster. The CH_3OH molecule still maintains its structural integrity. The property of the CH_3OH molecule to retain its original geometry is important for the applications of these clusters in nano-devices such as sensor molecule in order to probe cluster properties.[62] After adsorption, most Au—Au bond-lengths near adsorption site are elongated and only a few far from the adsorption site are shortened to some extent. Compared with free CH_3OH molecule, the O—H bond-length in hydroxyl group is elongated and the C—H bond-length in methyl group is shortened. Meanwhile, the C—O bond length between the hydroxyl group and methyl group becomes longer obviously. That's to say, the stability of CH_3 is strengthened and the stability of OH is weakened, the interaction between methyl group and hydroxyl group is also obviously weakened. As two relatively stable units in CH_3OH molecule, the methyl group and hydroxyl group become easy to participate in reactions. The reactivity enhancement of CH_3OH molecule can be observed

clearly. The bond-lengths of the lowest energy geometries for Au_3CH_3OH and Au_5CH_3OH clusters are very close to the results in Ref. [32] (deviations are less than 1%), and the Au—O, C—O bond-lengths for Au_4CH_3OH and Au_8CH_3OH clusters are also close to the values of 2.170 Å and 1.460 Å in Ref. [33]. The pictures of geometrical structures for these clusters are consistent with previous works.[32,33] Compared with the corresponding lowest energy geometry, the low-lying geometric isomers formed by bonding gold cluster with oxygen of methanol molecule at another adsorption site or by bonding gold cluster with hydrogen of hydroxyl group have longer Au—O bond-length or Au—H bond-length, shorter C—O bond-length, longer O—H bond-length and C—H bond-length. Meanwhile, much shorter Au—H bond-length and C—O bond-length, shorter O—H bond-length and much longer C—H bond-length also can be observed in the low-lying geometric isomers formed by bonding gold cluster with hydrogen of methyl group. The energy difference between the lowest energy geometry and its isomer is less than 1.000 eV, indicating that these isomers with slightly higher energy may also exist with some probability in the adsorption process of gold cluster toward methanol molecule.

3.2. Energy Analysis

To gain insight into the stability of pure Au_n clusters and Au_nCH_3OH ($n = 1$–13) clusters, the adsorption energy (E_{ad}), average binding energy per atom (E_b), the second-order difference of energy $\Delta_2E(n)$, HOMO–LUMO gap (HLG), vertical ionization potentials (VIP) and vertical electron affinity (VEA) for lowest energy geometry of pure Au_n clusters and Au_nCH_3OH clusters are evaluated by using the following equations:

$$E_{ad}(Au_nCH_3OH) = [E(Au_n) + E(CH_3OH) - E(Au_nCH_3OH)]$$

$$E_b(Au_n) = [nE(Au) - E(Au_n)]/n$$

$$E_b(Au_nCH_3OH) = [nE(Au) + E(C) + E(O) + 4E(H) - E(Au_nCH_3OH)]/(n+6)$$

$$\Delta_2E(n) = E(Au_{n+1}) + E(Au_{n-1}) - 2E(Au_n)$$

$$\Delta_2E(n) = E(Au_{n+1}CH_3OH) + E(Au_{n-1}CH_3OH) - 2E(Au_nCH_3OH)$$

$$VIP = E(Au_n)^+ - E(Au_n)$$

$$VIP = E(Au_nCH_3OH)^+ - E(Au_nCH_3OH)$$

$$VEA = E(Au_n) - E(Au_n)^-$$

$$VEA = E(Au_nCH_3OH) - E(Au_nCH_3OH)^-$$

From the adsorption energy displayed in Figure 2, we can see that with increasing number of gold atoms, the adsorption energies fluctuate in a wave-like manner with

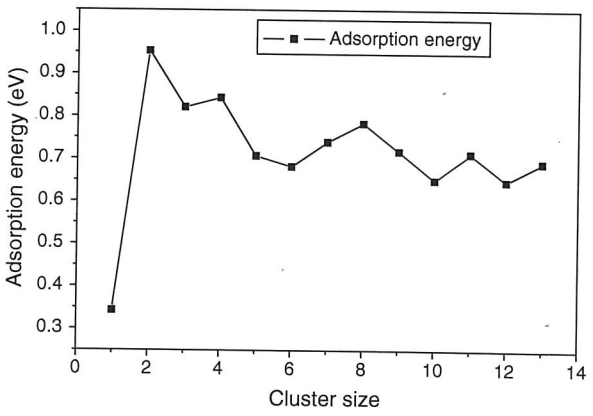

Figure 2. Size dependence of adsorption energy for Au_nCH_3OH clusters.

the opposite variation tendency of Au—O bond lengths and reach the maximum value of 0.953 eV at $n = 2$ and the minimum value of 0.343 eV at $n = 1$. This situation is consistent with the shortest Au—O bond-length in Au_2CH_3OH cluster and longest Au—O bond-length in $AuCH_3OH$ cluster. It is proved that the strongest adsorption exists in Au_2CH_3OH cluster and the weakest adsorption exists in $AuCH_3OH$ cluster. An inverse correlation between the Au—O bond-length and adsorption energy can be observed clearly (see Figs. 2 and 3). The adsorption energy values of 0.821 eV and 0.707 eV for Au_3CH_3OH cluster and Au_5CH_3OH cluster are higher than the values of 0.730 eV and 0.620 eV in Ref. [32]. This discrepancy may be explained in terms of the strong relativistic effect in gold clusters[37–40] without including in this previous work,[32] and also proves again that the relativistic effect might have obvious influence on the adsorption behavior of gold clusters.

From the average binding energy curves for Au_nCH_3OH and Au_n clusters displayed in Figure 4, we can find that the average binding energy of Au_nCH_3OH cluster is larger than that of corresponding pure Au_n cluster. With increasing number of gold atoms, the average binding energy of

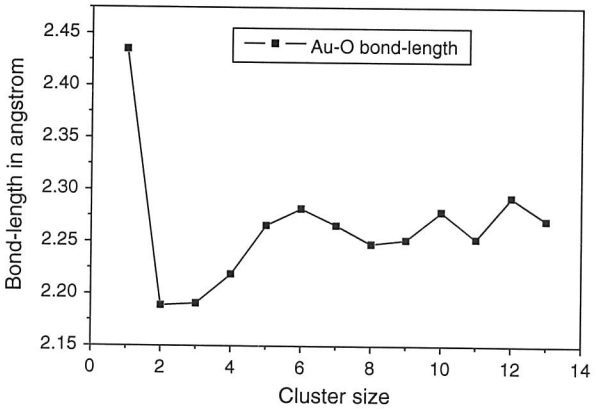

Figure 3. Size dependence of Au—O bond-length for Au_nCH_3OH clusters.

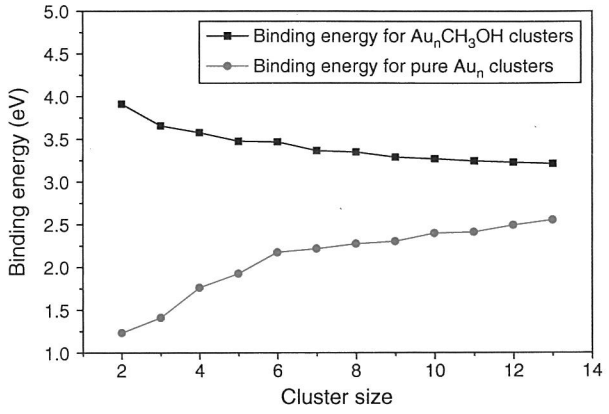

Figure 4. Size dependence of average binding energy for pure Au_n clusters and Au_nCH_3OH clusters.

pure Au_n cluster increases gradually and reaches the maximum value of 2.553 eV at $n = 13$. Meanwhile, the average binding energy of Au_nCH_3OH cluster also increases gradually and reaches the maximum value of 3.209 eV at $n = 13$ too. In addition, with increasing cluster size, the binding energy difference between Au_nCH_3OH and Au_n cluster becomes small gradually, an asymptotic increase (decrease) can seen clearly. As a measurement of cluster thermodynamic stability, above characteristics indicate that the thermodynamic stability of cluster is enhanced after adsorption. With increasing of cluster size, the stability of Au_nCH_3OH cluster is increased gradually like the increasing stability of pure Au_n cluster. But, the thermodynamic stability enhancement effect of methanol molecule adsorption becomes weakened gradually with increasing size of Au_nCH_3OH cluster.

In cluster physics, the second-order difference of cluster energies $\Delta_2E(n)$ is an extremely sensitive quantity that reflects the relative stability of cluster.[63] As a function of cluster size, the $\Delta_2E(n)$ of pure Au_n clusters and Au_nCH_3OH clusters displayed in Figure 5 exhibits same common odd-even oscillations. The second-order difference of cluster energies for even-numbered pure Au_n

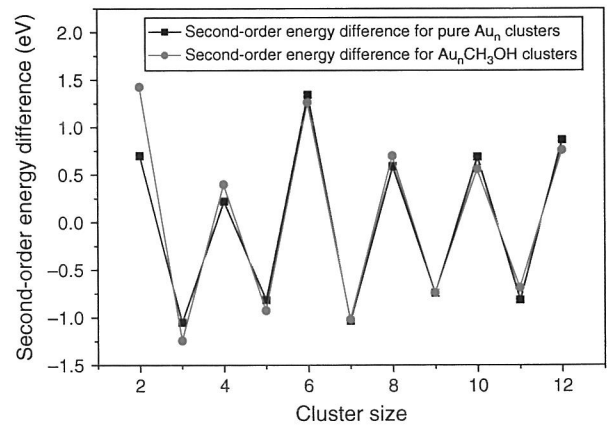

Figure 5. Size dependence of second-order energy difference for pure Au_n clusters and Au_nCH_3OH clusters.

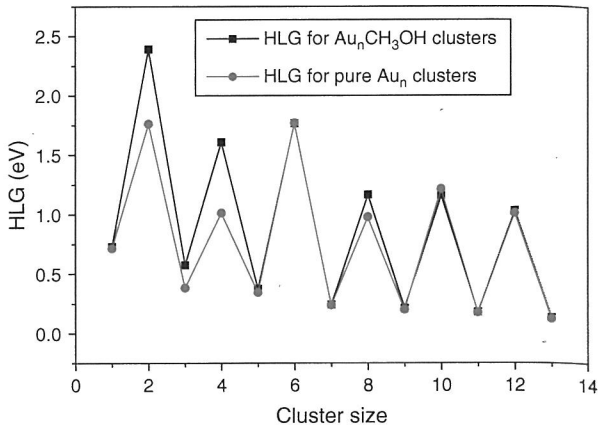

Figure 6. Size dependence of HLG for pure Au_n clusters and Au_nCH_3OH clusters.

cluster and Au_nCH_3OH cluster are larger than those for adjacent odd-numbered pure Au_n cluster and Au_nCH_3OH cluster, indicating that the even-numbered pure Au_n cluster and Au_nCH_3OH cluster are relatively more stable than the neighboring odd-numbered pure Au_n cluster and Au_nCH_3OH cluster. The relative stability of Au_nCH_3OH cluster is largely determined by the electronic structure of gold cluster with half-filled bands of nearly free *s* electrons, and the adsorption process has no influence on the relative stability of these clusters.

HOMO–LUMO gap (HLG) is a useful parameter for examining the electronic stability of a cluster. The larger of HLG, the higher energy is required to excite the electrons from valence band to conduction band, corresponding to higher stability of electronic structure. In Figure 6, an obvious odd-even oscillation of HLG for pure Au_n cluster and Au_nCH_3OH cluster can be observed clearly. It is inferred that the electronic structure of even-numbered pure Au_n cluster and Au_nCH_3OH cluster is more stable than that of neighboring odd-numbered pure Au_n cluster and Au_nCH_3OH cluster. The HLG value of Au_nCH_3OH ($n = 2$, 4 and 8) cluster is larger than that of corresponding

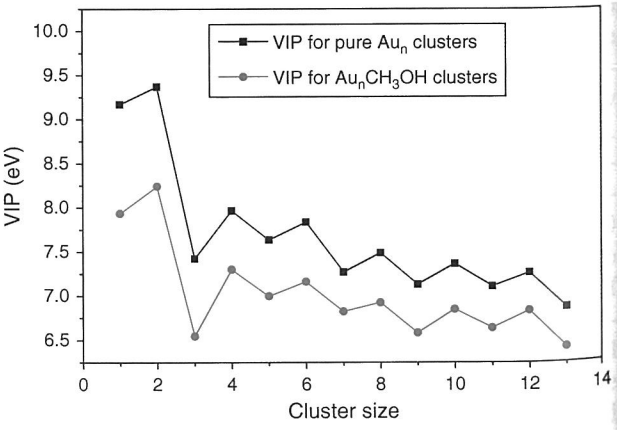

Figure 7. Size dependence of VIP for pure Au_n clusters and Au_nCH_3OH clusters.

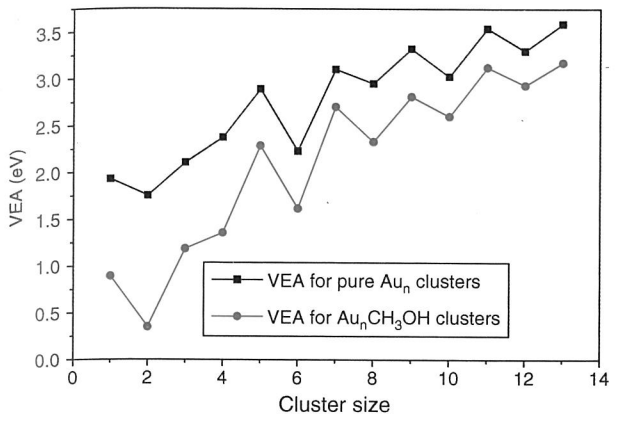

Figure 8. Size dependence of VEA for pure Au_n clusters and Au_nCH_3OH clusters.

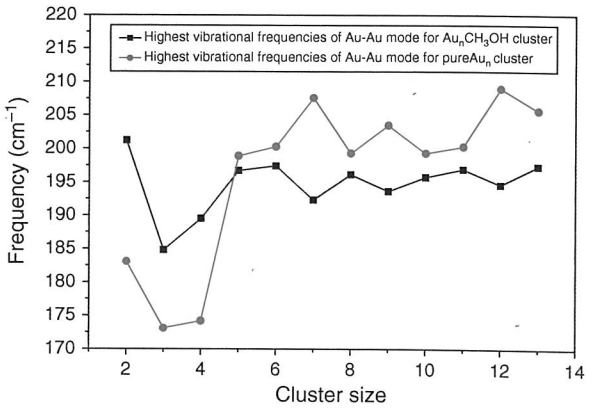

Figure 10. Highest vibrational frequencies of Au—Au mode for pure Au_n cluster and Au_nCH_3OH clusters.

pure Au_n ($n = 2$, 4 and 8) cluster, and the HLG value of other Au_nCH_3OH cluster is very close to that of corresponding pure Au_n cluster. It is suggested that the adsorption of methanol molecule may strengthen the electronic stability of Au_nCH_3OH ($n = 2$, 4 and 8) cluster and almost has no influence on the electronic stability of other Au_nCH_3OH cluster.

In addition to above parameters, the maximum hardness principle (MHP) also can be used to characterize the chemical stability of a cluster.[64, 65] In density functional theory, using the finite difference approximation and the Koopmans' theorem, chemical hardness η can be approximated as

$$\eta = \frac{\mathrm{VIP} - \mathrm{VEA}}{2}$$

where the VIP and VEA are vertical ionization potential and vertical electron affinity of the chemical system.[64–67]

Combining use the calculation results of VIP and VEA displayed in Figures 7 and 8, the chemical hardness for the lowest energy structures of pure Au_n and Au_nCH_3OH clusters are calculated and shown in Figure 9. It is easy to be found that the VIP and VEA of Au_nCH_3OH cluster are smaller than those of corresponding pure Au_n cluster. That is to say, after adsorption of CH_3OH molecule, less energy for one electron ionization is required and also less energy is released when an electron is added to a neutral cluster. The production of the corresponding cation is more easily to be realized and the production of the corresponding anion is not readily to be accomplished. Meanwhile, we can also find that the value of chemical hardness η of Au_nCH_3OH clusters is close to that of corresponding pure Au_n cluster. As the cluster size increases, a common odd-even oscillation of chemical hardness for pure Au_n cluster and Au_nCH_3OH clusters also can be observed clearly. This picture is consistent well with odd-even oscillations of second-order difference of cluster energies (see Fig. 5) and HLGs (see Fig. 6). According to the maximum hardness principle (MHP),[64, 65] it proves that no obvious changes for the chemical stability of cluster can be observed after adsorption, the even-numbered pure Au_n cluster and Au_nCH_3OH clusters with higher chemical hardness are relatively more stable than the neighboring odd-numbered pure Au_n cluster and Au_nCH_3OH cluster with lower chemical hardness.

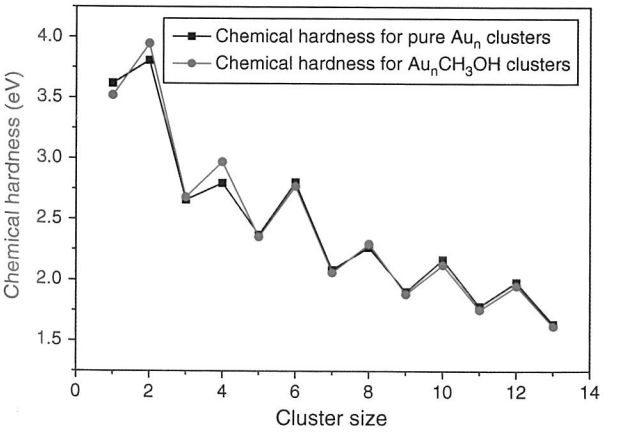

Figure 9. Size dependence of chemical hardness for pure Au_n clusters and Au_nCH_3OH clusters.

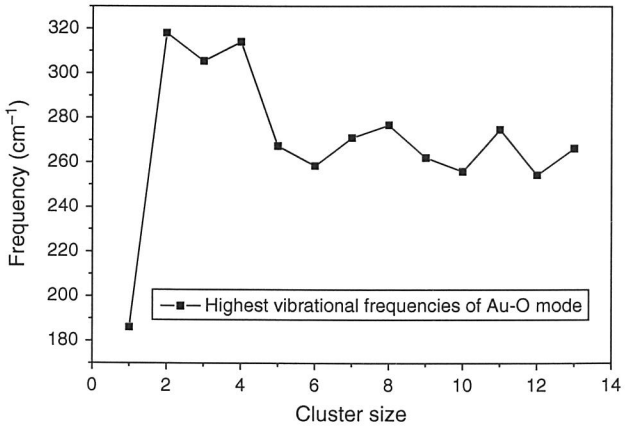

Figure 11. Highest vibrational frequencies of Au—O mode for Au_nCH_3OH clusters.

Table I. Calculated highest vibrational frequencies of C—O, C—H and O—H mode for Au_nCH_3OH clusters and single CH_3OH molecule.

Cluster	ω_{C-O} (cm^{-1})	ω_{C-H} (cm^{-1})	ω_{O-H} (cm^{-1})	Cluster	ω_{C-O} (cm^{-1})	ω_{C-H} (cm^{-1})	ω_{O-H} (cm^{-1})
CH_3OH	1471.0	3046.0	3766.6	Au_7CH_3OH	1322.9	3151.1	3693.5
$AuCH_3OH$	1321.4	3143.5	3695.2	Au_8CH_3OH	1327.8	3156.2	3700.6
Au_2CH_3OH	1330.4	3161.6	3706.5	Au_9CH_3OH	1327.6	3167.7	3701.2
Au_3CH_3OH	1330.4	3172.3	3706.6	$Au_{10}CH_3OH$	1319.0	3144.9	3690.7
Au_4CH_3OH	1322.7	3168.1	3719.4	$Au_{11}CH_3OH$	1317.9	3151.2	3691.4
Au_5CH_3OH	1326.1	3148.2	3703.5	$Au_{12}CH_3OH$	1322.4	3152.8	3702.8
Au_6CH_3OH	1327.1	3157.3	3704.3	$Au_{13}CH_3OH$	1327.4	3164.1	3707.7

3.3. Frequency Analysis

The vibrational frequency is another important parameter to check the interaction between bonded atoms, and higher vibrational frequency often corresponds to the stronger interaction between the specified bonded atoms. By frequency analysis, the highest vibrational frequencies of Au—Au mode for the lowest energy geometries of pure Au_n clusters and Au_nCH_3OH clusters are depicted in Figure 10 comparatively. Meanwhile, the highest frequencies of Au—O, C—O, C—H and O—H mode for Au_nCH_3OH clusters and single CH_3OH molecule are given in Figure 11 and Table I, respectively. Obviously, the highest vibrational frequency of Au—Au mode for Au_nCH_3OH ($n = 2$–4) clusters is higher than that of Au—Au mode for corresponding Au_n cluster, and however the highest vibrational frequency of Au—Au mode for other Au_nCH_3OH clusters is lower than that of Au—Au mode for corresponding Au_n cluster. It is inferred that some Au—Au interactions in Au_nCH_3OH ($n = 2$–4) clusters may be strengthened and the Au—Au interactions in other Au_nCH_3OH clusters are weakened. Meanwhile, we can also find that the variation tendency of Au—O vibrational frequency for Au_nCH_3OH clusters is consistent well with the variation tendency of adsorption energy. Higher vibrational frequency of Au—O mode means stronger Au—O interaction, and also corresponds to shorter Au—O bond-length and stronger adsorption. In addition, it is easy to be found that the highest vibrational frequencies of C—O mode and O—H mode for Au_nCH_3OH cluster are lower than those of C—O mode and O—H mode for free CH_3OH molecule, and the highest vibrational frequency of C—H mode for Au_nCH_3OH cluster is higher than that of C—H mode for free CH_3OH molecule. It is suggested that the CH_3—OH interaction and the O—H interaction in hydroxyl group becomes weak, the C—H interaction becomes strong. This situation is consistent with the longer C—O bond-length, shorter C—H bond-length and longer O—H bond-length in the lowest energy geometry of Au_nCH_3OH clusters. It also proves again that the chemical activities of hydroxyl group and methyl group are enhanced to some extent after adsorption.

3.4. Electronic and Magnetic Properties

In order to understand the nature of chemical bonding in these systems, we have plotted the spatial orientation of the highest occupied molecular orbital (HOMO), the lowest

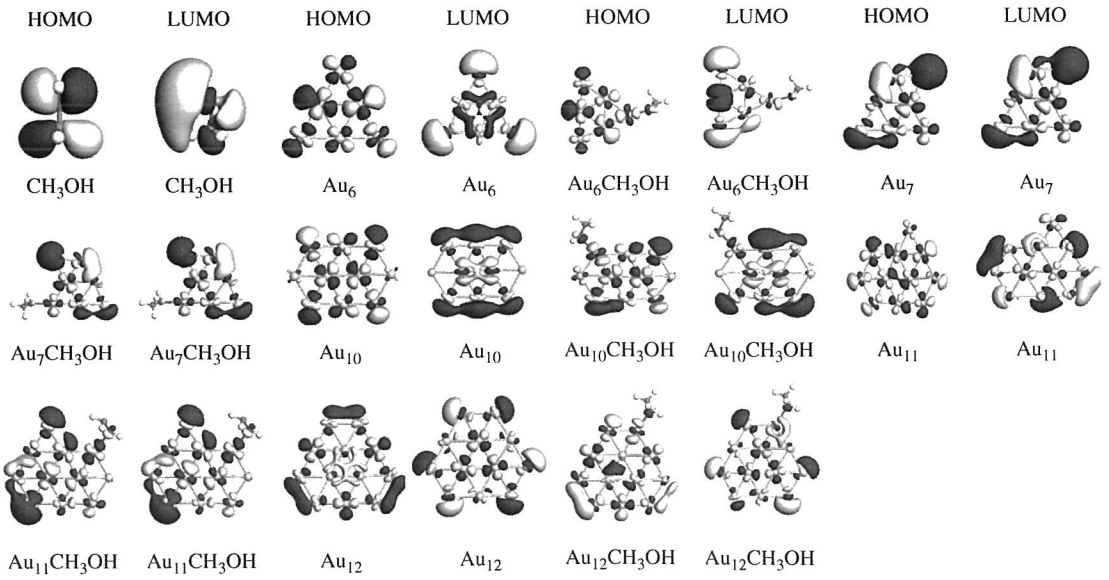

Figure 12. Spatial orientations of HOMO and LUMO with isosurface value 0.03 for some representative pure Au_n clusters, Au_nCH_3OH clusters and CH_3OH molecule.

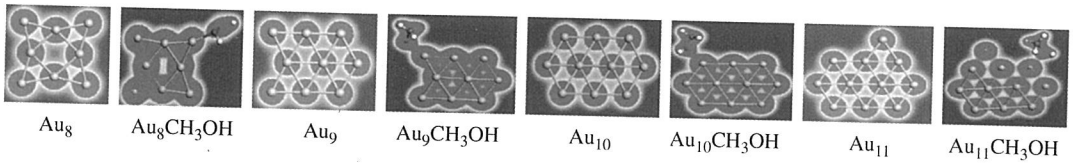

Figure 13. Electron densities in the cluster plane for some representative pure Au_n clusters and Au_nCH_3OH clusters, the color scale bar is given at the top of this figure.

unoccupied molecular orbital (LUMO) and the electron densities in the cluster plane for some representative pure Au_n clusters and Au_nCH_3OH clusters in Figures 12 and 13 comparatively. At first glance, the HOMO and LUMO of Au_n part for pure Au_n cluster and Au_nCH_3OH cluster are similar and delocalized obviously with a contribution from almost all gold atoms in the cluster. This picture may be explained in terms of the strong scalar relativistic effect in small gold cluster[37–40] and also tells us that the influence of adsorption toward methanol molecule on the frontier orbital is slight. Meanwhile, different from single CH_3OH molecule which the contributions of all atoms to HOMO and LUMO can be seen clearly, the contribution of CH_3OH seldom appears in the HOMO and LUMO of Au_nCH_3OH clusters due to its low orbital energy. CH_3OH molecule adsorption onto a gold cluster can be seen that it is only partly involving the excitation of formerly unoccupied orbital in the cluster, since the open shell has to be "pushed up" when the Au—O bond is formed. The same argument also can be found in connection with the bond preparation method used in the cluster surface model.[68] Additionally, in Figure 13, compared with electron cloud overlap between Au atoms in corresponding Au_n cluster, more electron cloud overlap between Au atoms or between Au and CH_3OH in Au_nCH_3OH cluster can be found. Besides the strong *sd* hybridization in Au atoms or between two Au atoms in Au_n, the *spd* hybridization between Au_n and CH_3OH in Au_nCH_3OH clusters also can be observed. The unpaired electrons in Au_n may have more chance to be paired with the valence electrons of CH_3OH.

To further understand the electronic properties of Au_nCH_3OH clusters, in Table II, we perform a detailed Mulliken population analysis of charge transfer from CH_3OH to Au_n and from CH_3 to OH for the lowest energy geometries. The values of charge transfers suggest

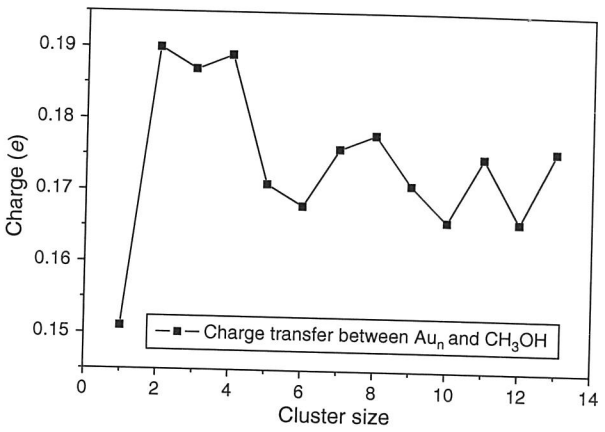

Figure 14. Charge transfer between Au_n and CH_3OH in Au_nCH_3OH clusters.

a mechanism to favor of electron donation, that is, charge transfer from CH_3OH to Au_n, the Au_n behaves as an electron acceptor in the reaction. This situation can be explained in terms of the electron donation from the $p\pi$ orbital of CH_3OH to the $d\sigma + sp$ hybridized orbital of Au and the electron back donation from the occupied $d\pi$ orbital of Au to the unoccupied $p\pi$ orbital of CH_3OH molecule, which results the better overlap of these orbitals and the enhancement of gold—oxygen bonding. To some extent, we can say that the mechanism of charge transfer between atoms might influence the bonding of these two specified atoms. The larger of the charge transfer, which results in a stronger hybridization with the host, the stronger of the specified bonding. It is easy to see that the variation tendency of charge transfer between CH_3OH and Au_n is consistent well with the variation tendency of adsorption energy (see Figs. 2 and 14), and the relatively larger charge transfers between CH_3OH and Au_n take place in Au_nCH_3OH clusters ($n = 2$–4), corresponding

Table II. Calculated charge transfer from CH_3OH to Au_n and from CH_3 to OH for the lowest energy geometries of Au_nCH_3OH clusters.

Cluster	Charge (e)			Cluster	Charge (e)		
	Au_n	CH_3	OH		Au_n	CH_3	OH
CH_3OH		0.248	−0.248	Au_7CH_3OH	−0.176	0.344	−0.168
$AuCH_3OH$	−0.151	0.308	−0.157	Au_8CH_3OH	−0.178	0.349	−0.171
Au_2CH_3OH	−0.190	0.352	−0.162	Au_9CH_3OH	−0.171	0.337	−0.166
Au_3CH_3OH	−0.187	0.355	−0.168	$Au_{10}CH_3OH$	−0.166	0.337	−0.171
Au_4CH_3OH	−0.189	0.347	−0.158	$Au_{11}CH_3OH$	−0.175	0.342	−0.167
Au_5CH_3OH	−0.171	0.341	−0.170	$Au_{12}CH_3OH$	−0.166	0.334	−0.168
Au_6CH_3OH	−0.168	0.344	−0.176	$Au_{13}CH_3OH$	−0.176	0.344	−0.168

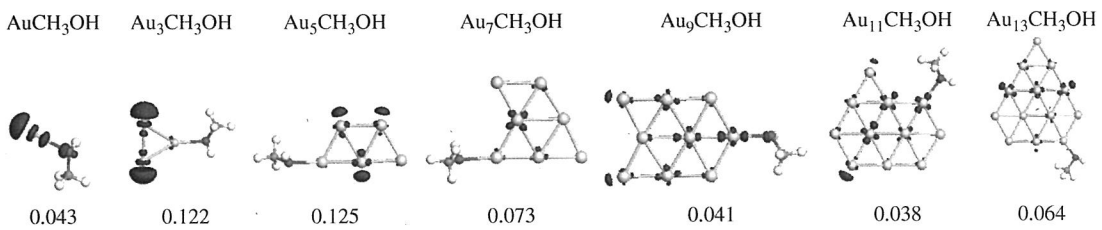

Figure 15. Spatial orientations of spin density for odd-numbered Au_nCH_3OH clusters, the isosurface values are shown next to each cluster.

to the larger adsorption energies and shorter Au—O bond-lengths. Meanwhile, we can also find that the charge transferred from CH_3 to OH in Au_nCH_3OH clusters is obviously smaller than that in single CH_3OH, indicating that the CH_3—OH bonding in Au_nCH_3OH is obviously weakened, the reactivity enhancement of CH_3OH might be expected after adsorption.

From Figure 1, we can see that all the Au_nCH_3OH clusters prefer low spin multiplicity ($M = 1$ for even-numbered Au_nCH_3OH clusters, $M = 2$ for odd-numbered Au_nCH_3OH clusters). The even-numbered Au_nCH_3OH clusters are found to exhibit zero magnetic moment, and the odd-numbered Au_nCH_3OH clusters are found to possess magnetic moment with the value of 1 μ_B. The magnetic moments are mainly contributed by gold atoms in these odd-numbered Au_nCH_3OH clusters (see Fig. 15). Meanwhile, the HOMOs of even-numbered Au_nCH_3OH clusters with even number of valence electrons are fully occupied by the majority spin and minority spin electrons, which leads to the ground state of these clusters with closed electronic shells and are stable remarkably. But, the HOMOs of odd-numbered Au_nCH_3OH clusters with odd number of valence electrons are occupied partially only by majority spin electrons or minority spin electrons and have open electronic shells (see Table III). According to the Jahn-Teller theorem,[69, 70] these odd-numbered Au_nCH_3OH clusters with open electronic shell have the tendency to distort further toward lower symmetry in order to reduce or to remove the degeneracy and lower the energy. This possibility of Jahn-Teller distortion tells us that the odd-numbered Au_nCH_3OH clusters might be less stable chemically and electronically compared with the even-numbered Au_nCH_3OH clusters. It is also consistent well with odd-even oscillations of second-order difference of cluster energies (see Fig. 5) and HLGs (see Fig. 6).

Table III. Electronic configurations and $\langle S^2 \rangle$ values for the lowest energy geometries Au_nCH_3OH clusters.

Cluster	$\langle S^2 \rangle$	Electronic configuration	Cluster	$\langle S^2 \rangle$	Electronic configuration
CH_3OH	0.000	Closed	Au_7CH_3OH	0.819	Open
$AuCH_3OH$	0.754	Open	Au_8CH_3OH	0.015	Closed
Au_2CH_3OH	0.000	Closed	Au_9CH_3OH	0.794	Open
Au_3CH_3OH	0.752	Open	$Au_{10}CH_3OH$	0.013	Closed
Au_4CH_3OH	0.003	Closed	$Au_{11}CH_3OH$	0.810	Open
Au_5CH_3OH	0.794	Open	$Au_{12}CH_3OH$	0.028	Closed
Au_6CH_3OH	0.002	Closed	$Au_{13}CH_3OH$	0.798	Open

In DFT calculations, for open-shell systems, a solution of low spin state is often contaminated by higher spin states and this challenge problem is called spin-contamination. The spin unrestricted determinant with spin-contamination is not the accurate eigenfunction of total spin and thus some error may be introduced into the calculations.[71–74] As a check for the presence of spin contamination, we report the $\langle S^2 \rangle$ values for the lowest energy geometries of Au_nCH_3OH clusters in Table III. As we had expected, the $\langle S^2 \rangle$ values for the even-numbered Au_nCH_3OH clusters with singlet are close to zero and almost no spin-contaminations can be found in these closed-shell systems. The $\langle S^2 \rangle$ values for the open-shell systems of odd-numbered Au_nCH_3OH clusters are slightly larger than the exact value of 0.75 for doublet and the deviations are less than 10%. It is suggested that the influences of spin-contamination in these open shell systems of odd-numbered Au_nCH_3OH clusters are still in a small scales and can be acceptable.

4. CONCLUSIONS

In this paper, an all-electron scalar relativistic calculation on the adsorption of Au_n ($n = 1$–13) clusters toward methanol molecule has been performed by using density functional theory with the generalized gradient approximation at PW91 level. The main conclusions are summarized as follows:

(1) The small gold cluster would like to bond with oxygen of methanol molecule at the edge of gold cluster plane, the CH_3OH molecule prefers to occupy the on-top and single fold coordination site. After adsorption, the O—H bond-length in hydroxyl group is elongated and the C—H bond-length in methyl group is shortened. Meanwhile, the C—O bond length between the hydroxyl group and methyl group becomes longer obviously. The chemical activities of hydroxyl group and methyl group are enhanced to some extent.

(2) After adsorption, the thermodynamic stability of cluster is strengthened, but, no obvious changes for the chemical stability of cluster can be observed. The even-numbered Au_nCH_3OH cluster with closed-shell electronic configuration is relatively more stable than the neighboring odd-numbered Au_nCH_3OH cluster with open-shell electronic configuration.

(3) All the Au_nCH_3OH clusters prefer low spin multiplicity ($M = 1$ for even-numbered Au_nCH_3OH clusters, $M = 2$

for odd-numbered Au_nCH_3OH clusters) and the magnetic moments are mainly contributed by gold atoms.

Acknowledgments: This work is supported by the Doctoral Foundation of Southwest University of Science and Technology. No. 12zx701.

References and Notes

1. R. Parsons and T. Vandernoot, *J. Electroanal. Chem.* 257, 9 (**1988**).
2. M. Konopka, R. Rousseau, I. Stich, and D. Marx, *J. Am. Chem. Soc.* 126, 12103 (**2004**).
3. K. Bhattacharya, A. K. Tripathi, and G. K. Dey, *J. Nanosci. Nanotech.* 5, 790 (**2005**).
4. N. D. Shinn, *Surf. Sci.* 278, 157 (**1992**).
5. J. S. Huberty and J. R. J. Madix, *Surf. Sci.* 360, 144 (**1996**).
6. S. R. Bare, J. A. Stroscio, and W. Ho, *Surf. Sci.* 150, 399 (**1985**).
7. J. P. Camplin and E. M. McCash, *Surf. Sci.* 360, 229 (**1996**).
8. S. L. Silva, R. M. Lemor, and F. M. Leibsle, *Surf. Sci.* 421, 135 (**1999**).
9. W. S. Sim, P. Gardner, and D. A. King, *J. Phys. Chem.* 99, 16002 (**1995**).
10. J. J. Chen, Z. C. Jiang, Y. Zhou, B. R. Chakraborty, and N. Winograd, *Surf. Sci.* 328, 248 (**1995**).
11. M. Endo, T. Matsumoto, J. Kubota, K. Domen, and C. Hirose, *Surf. Sci.* 441, L931 (**1999**).
12. J. R. B. Gomes and J. Gomes, *Surf. Sci.* 471, 59 (**2001**).
13. J. R. B. Gomes, J. Gomes, and F. Illas, *J. Mol. Catal. A: Chem.* 170, 187 (**2001**).
14. A. H. Jones, S. Poulston, R. A. Bennett, and M. Bowker, *Surf. Sci.* 380, 31 (**1997**).
15. J. Greeley and M. Mavrikakis, *J. Catal.* 208, 291 (**2002**).
16. J. Greeley and M. Mavrikakis, *J. Am. Chem. Soc.* 124, 7193 (**2002**).
17. M. Okumura, S. Nakamura, S. Tsubota, T. Nakamura, M. Azuma, and M. Haruta, *Catal. Lett.* 51, 53 (**1998**).
18. G. C. Bond and D. Thompson, *Catal. Rev. Sci. Eng.* 41, 319 (**1999**).
19. M. Valden, X. Lai, and D. W. Goodman, *Science* 281, 1647 (**1998**).
20. M. Harut, *Chem. Rec.* 3, 75 (**2000**).
21. M. C. Daniel and D. Astruct, *Chem. Rev.* 104, 293 (**2004**).
22. X. J. Xu, J. J. Li, and X. M. Liu, *J. Nanosci. Nanotech.* 6, 872 (**2006**).
23. N. Bogdanchikova, L. Tuzovskaya, and A. Pestryakov, *J. Nanosci. Nanotech.* 11, 5476 (**2011**).
24. M. Haruta, N. Yamada, T. Kobayashi, and S. Iijima, *J. Catal.* 115, 310 (**1989**).
25. F. Boccuzzi and A. J. Chiorino, *Phys. Chem. B* 104, 5414 (**2000**).
26. H. Hakkinen and U. Landman, *J. Am. Chem. Soc.* 123, 9704 (**2001**).
27. W. T. Wallace and R. W. Whetten, *J. Am. Chem. Soc.* 124, 7499 (**2002**).
28. N. Lopez and J. K. Norskov, *J. Am. Chem. Soc.* 124, 11262 (**2002**).
29. L. M. Molina and B. Hammer, *Phys. Rev. Lett.* 90, 206102 (**2003**).
30. M. L. Kimble, A. W. Castleman, R. Mitric, C. Burgel, and V. Bonacic-Koutecky, *J. Am. Chem. Soc.* 126, 2526 (**2004**).
31. J. Botana, M. Pereiro, and D. Baldomir, *J. Nanosci. Nanotech.* 10, 2787 (**2010**).
32. Y. C. Li, C. L. Yang, M. Y. Sun, X. X. Li, Y. P. An, M. S. Wang, X. G. Ma, and D. H. Wang, *J. Phys. Chem. A* 113, 1353 (**2009**).
33. R. Rousseau and D. Marx, *J. Chem. Phys.* 112, 761 (**2000**).
34. G. Dietrich, S. Krückeberg, K. Lützenkirchen, L. Schweikhard, and C. Walther, *J. Chem. Phys.* 112, 752 (**2000**).
35. R. Rousseau, G. Dietrich, S. Kruckeberg, K. Lutzenkirchen, D. Marx, L. Schweikhard, and C. Walther, *Chem. Phys. Lett.* 295, 41 (**1998**).
36. C. R. Chang, X. F. Yang, B. Long, and J. Li, *ACS Catal.* 3, 1693 (**2013**).
37. P. Pyykko, *Chem. Rev.* 88, 563 (**1988**).
38. E. M. Fernandez, J. M. Soler, L. L. Garzon, and C. Balbas, *Phys. Rev. B* 70, 165403 (**2004**).
39. R. Wesendrup, T. Hunt, and P. Schwerdtfeger, *J. Chem. Phys.* 112, 9356 (**2000**).
40. J. Autschbach, S. Siekierski, M. Seth, P. Schwerdtfeger, and W. H. E. Schwarz, *J. Compu. Chem.* 23, 804 (**2002**).
41. X. J. Kuang, X. Q. Wang, and G. B. Liu, *J. Chem. Sci.* 125, 401 (**2013**).
42. X. J. Kuang, X. Q. Wang, and G. B. Liu, *Physica E-Low-Dimensional Systems and Nanostructures* 40, 2132 (**2012**).
43. B. Delley, *J. Chem. Phys.* 92, 508 (**1990**).
44. B. Delley, *J. Chem. Phys.* 113, 7756 (**2000**).
45. J. P. Perdew and Y. Wang, *Phys. Rev. B* 45, 13244 (**1992**).
46. B. Delley, *Phys. Rev. B* 66, 155125 (**2002**).
47. M. S. Phala, G. Klatt, and E. V. Steen, *Chem. Phys. Lett.* 395, 33 (**2004**).
48. X. J. Kuang, X. Q. Wang, and G. B. Liu, *Cata. Lett.* 137, 137 (**2010**).
49. X. J. Kuang, X. Q. Wang, and G. B. Liu, *Euro. Phys. J. D.* 61, 71 (**2011**).
50. X. J. Kuang, X. Q. Wang, and G. B. Liu, *App. Surf. Sci.* 257, 6546 (**2011**).
51. A. Deka and R. C. Deka, *J. Mol. Struct.: Theochem.* 870, 83 (**2008**).
52. B. Assadollahzadeh and P. Schwerdtfeger, *J. Chem. Phys.* 131, 064306 (**2009**).
53. J. Ho, K. M. Ervin, and W. C. Lineberger, *J. Chem. Phys.* 93, 6987 (**1990**).
54. B. Simard and P. A. Hackett, *J. Mol. Spectrosc.* 142, 310 (**1990**).
55. L. L. Ames and R. F. Barrow, *Trans. Faraday. Soc.* 63, 39 (**1967**).
56. C. Jackslath, I. Rabin, W. Schulze and B. Bunsenges, *Phys. Chem.* 96, 1200 (**1992**).
57. S. Hirabayashi, R. Okawa, M. Ichihashi, T. Kondow, and Y. Kawazoe, *J. Phys. Chem. A* 111, 7664 (**2007**).
58. M. Ichihashi, C. A. Corbett, T. Hanmura, J. M. Lisy, and T. Kondow, *J. Phys. Chem. A* 109, 7872 (**2005**).
59. T. Shimanouchi, Tables of Molecular Vibrationl Frequencies, National Bureau of Standards Reference Data Series, NBS, Washington, DC (**1972**), Vol. I.
60. G. P. Li and I. P. Hamilton, *Chem. Phys. Lett.* 420, 474 (**2006**).
61. H. W. Ghebriel and A. Kshirsagar, *J. Chem. Phys.* 126, 244705 (**2007**).
62. R. Rousseau, G. Dietrich, S. Krckeberg, K. Lutzenkirchen, D. Marx, L. Schweikhard, and C. Walther, *Chem. Phys. Lett.* 295, 41 (**1998**).
63. C. C. Wang, R. N. Zhao, and J. G. Han, *J. Chem. Phys.* 124, 194301 (**2006**).
64. R. G. Parr and P. K. Chattaraj, *J. Am. Chem. Soc.* 113, 1854 (**1991**).
65. R. G. Pearsom, *J. Chem. Educ.* 64, 561 (**1987**).
66. K. Fukui, *Science* 218, 747 (**1982**).
67. J. G. He, K. G. Wu, C. P. Liu, and R. G. Sa, *Chem. Phys. Lett.* 483, 30 (**2009**).
68. L. Panas, P. Siegbahn, and U. Walhgren, *Chem. Phys.* 112, 325 (**1987**).
69. M. E. Eberhart, R. C. Handley, and K. H. Johnson, *Phys. Rev. B* 29, 1097 (**1984**).
70. J. L. Yang, F. Toigo, and K. L. Wang, *Phys. Rev. B* 50, 7915 (**1994**).
71. K. Yamaguchi, R. Carbo, and M. Klobukowski (eds.), Self-Consistent Field Theory and Applications, Elsevier, Amsterdam (**1990**), p. 727.
72. A. Szabo and N. S. Ostlund, Modern Quantum Chemistry, Dover Publications, Inc., New York, NY (**1996**), Chap. 3, pp. 205–230.
73. K. Yamaguchi, T. Kawakami, Y. Takano, Y. Kitagawa, Y. Yamashita, and H. Fujita, *Int. J. Quantam. Chem.* 90, 370 (**2002**).
74. B. Hajgató, D. Szieberth, P. Geerlings, F. DeProft, and M. S. Deleuze, *J. Chem. Phys.* 131, 224321 (**2009**).

Received: 27 August 2013. Accepted: 10 October 2013.